Reflex modulation and functional improvements following spinal cord stimulation for sensory restoration after lower-limb amputation

Ashley N Dalrymple*[1,2,3,4], Rohit Bose*[2,5,6], Devapratim Sarma[1,2], Bailey A Petersen[2,5,6,7], Beatrice Barra[2,8], Ameya C Nanivadekar[2,5,6], Tyler J Madonna[2,11], Monica F Liu[2,5,6,9,10], Isaiah Levy[2,11], Eric R Helm[11], Vincent J Miele[12], Marco Capogrosso[2,12], Lee E Fisher[2,5,6,11], Douglas J Weber[1,2,13]

*These authors contributed equally

1 Department of Mechanical Engineering, Carnegie Mellon University, Pittsburgh, PA, USA

2 Rehab Neural Engineering Labs, University of Pittsburgh, Pittsburgh, PA, USA

3 Department of Biomedical Engineering, University of Utah, Salt Lake City, UT, USA

4 Department of Physical Medicine and Rehabilitation, University of Utah, Salt Lake City, UT, USA

5 Department of Bioengineering, University of Pittsburgh, Pittsburgh, PA, USA

6 Center for Neural Basis of Cognition, Pittsburgh, PA, USA

7 Department of Critical Care Medicine, University of Pittsburgh, Pittsburgh, PA, USA

8 Neuroscience Institute, New York University Langone Health, New York, USA

9 Department of Physiology and Biophysics, Computational Neuroscience Center, University of Washington

10 Allen Institute, University of Washington

11 Department of Physical Medicine and Rehabilitation, University of Pittsburgh, Pittsburgh, PA, USA

12 Department of Neurological Surgery, University of Pittsburgh, Pittsburgh, PA, USA

13 Neuroscience Institute, Carnegie Mellon University, Pittsburgh, PA, USA

Corresponding author:

Douglas J Weber

dougweber@cmu.edu

5000 Forbes Ave, Wean 1323

Pittsburgh, PA, USA 15217

Key words: spinal cord stimulation, amputation, neural prosthesis, posterior root muscle reflexes, electromyography, pelvic obliquity

ABSTRACT

Background: The goal of this study was to characterize spinal reflexes and muscle activation in people with lower-limb amputation during use of a sensory neuroprosthesis. People with lower-limb amputations lack sensory inputs from their missing limb, which increases their risk of falling. People with lower-limb amputation exhibit co-contractions of antagonist muscles and reduced pelvic obliquity range-of-motion and pelvic drop. These motor functions are governed, in part, by sensory-mediated spinal reflexes; loss of somatosensation after amputation contributes to their dysfunction. Spinal cord stimulation (SCS) can restore sensation in the missing limb, but its effects on spinal reflex modulation and muscle activation have not been studied in people with lower-limb amputation.

Methods: We implanted percutaneous SCS electrodes over the lumbosacral enlargement in 3 people with trans-tibial amputation (2 diabetic neuropathy; 1 traumatic) for 28 or 84 days. SCS was used to restore sensation in the missing limb. We used electromyography (EMG) to record posterior root-muscle (PRM) reflexes and muscle activity of the residual limb. We characterized rate-dependent depression and recruitment properties of the PRM reflexes, measured changes in PRM amplitudes over time during quiet standing, and quantified changes in muscle activation and pelvic obliquity during walking with SCS over time.

Results: SCS evoked PRM reflexes in the residual limb muscles in all participants, which was confirmed by the presence of rate-dependent depression at stimulation frequencies ≥2Hz. Overall, there was broad activation of residual limb muscles with SCS. Sensations that were evoked exclusively in the residual limb were associated with a time-dependent increase in PRM reflex amplitude in proximal leg muscles; whereas sensations evoked the missing limb were associated with a progressive decrease in PRM reflex amplitude in all muscles except for medial gastrocnemius. During walking, co-contractions of knee antagonist muscles were reduced following multiple sessions of SCS-mediated sensory restoration. Additionally, the activation of the tensor fasciae latae muscle (hip abductor) increased during gait with SCS-mediated sensory restoration, which corresponded to an increase in pelvic obliquity range-of-motion and pelvic drop.

Conclusions: Restoring sensation in the missing limb using SCS modulates spinal reflexes, reduces co-contractions of antagonist muscles, and improves pelvic obliquity.

INTRODUCTION

By the end of 2050, it is estimated that over 3.6 million people in the United States will be living with a lower-limb amputation as a consequence of vascular disease (54%) or trauma (45%) [1,2]. People with a lower-limb amputation encounter significant challenges in maintaining stability while standing and walking, and as a result, are more likely to fall [3–6]. A primary reason for the higher incidence of falls among people with a lower-limb amputation is the lack of somatosensory feedback from the amputated limb and prosthesis [3,4]. Restoring somatosensation in the missing limb can improve stability during standing and walking [7–10].

Spinal cord stimulation (SCS) is an existing clinical neurotechnology that is used to treat chronic pain, including but not frequently phantom limb pain by stimulating the dorsal column of the spinal cord with electrodes implanted along the midline in the epidural space [11–14]. Recently, we demonstrated that by implanting SCS leads laterally in the epidural space, we can evoke sensations in the missing limb of people with a lower-limb amputation [10]. Laterally-placed SCS, excites the dorsal spinal roots containing sensory axons from proprioceptors (type Ia and Ib afferents) and mechanoreceptors (type II afferents) [15]. By exciting these afferent fibers, SCS engages spinal reflex pathways that innervate motoneurons. These spinal reflexes, known as posterior root-muscle (PRM) reflexes, can be recorded using electromyography (EMG) [16–18]. PRM reflexes are a compound reflex response resulting from the multi-segment activation of proprioceptive (type Ia, Ib) and cutaneous (type II) afferent fibers that synapse onto spinal motoneurons and interneurons [17,19,20].

By engaging spinal reflex pathway, somatosensory feedback from the feet and legs plays a crucial role in modulating muscle activity during standing and walking [21–23]. Specifically, somatosensory feedback from the legs facilitates limb loading during stance [24,25], regulates the transitions between the swing and stance phases of walking [26], and facilitates corrective responses to perturbations during walking [22,27,28]. Without this stream of sensory information from the periphery, the spinal sensorimotor mechanisms cannot effectively modulate the innate sensory-evoked reflex responses that are vital for maintaining stability during standing and walking.

Characterizing how spinal reflexes are altered following limb amputation and modulated using SCS to restore sensation in the missing limb is key to improve ambulatory function for people with a lower-limb amputation. Here, we characterize the PRM reflexes evoked by SCS in three individuals with transtibial amputation. We compare the activity of lower-limb muscles of the residual limb during sitting and standing with SCS, and walking with or without SCS, across the 30- or 90-day duration of the implant. We show that SCS evokes PRM reflexes in the lower-limb muscles as expected by the myotomal organization of the spinal cord and the rostral-caudal arrangement of the SCS electrodes. We report a reduction in co-contractions of the knee antagonist muscles following multiple weeks of SCS. Furthermore, after 3 months of SCS in one subject, we observed an increase in EMG during walking in the tensor fasciae latae muscle (hip abductor), which corresponded to an increase in pelvic obliquity range-of-motion and pelvic drop.

METHODS

All procedures were approved by the Institutional Review Board at the University of Pittsburgh and conformed to the Declaration of Helsinki. All participants provided written informed consent prior to their enrollment in the study. No participants had prior experience with SCS. Data

collected and reported in this study were part of another study investigating SCS to restore sensations in the missing limb, improve balance and gait function, and to reduce phantom limb pain [10].

Participants

Three individuals with transtibial amputations participated in this study (Table 1). All participants regularly used a non-motorized lower-limb prosthesis to walk for >40 months before implant. Participants 1 and 3 had an amputation due to complications from diabetic neuropathy and were limited community ambulators (determined by the Amputee Mobility Predictor). Participant 2 had a traumatic amputation and was an active community ambulator. The implant duration was 28 days in Participants 1 and 2 and 84 days in Participant 3. The extended implant duration in Participant 3 was performed under an Investigational Device Exemption from the United States Food and Drug Administration. Both studies are registered at ClinicalTrials.gov (NCT03027947 and NCT04547582).

Participant ID	Age	Gender	Years since amputation	Nature of amputation	Side of amputation	Ambulation level	Implant duration (days)
1	56-60	M	3.5	Diabetic	Left	Limited community	28
2	56-60	M	7	Traumatic	Left	Active	28
3	60-65	W	5	Diabetic	Left	Limited community	84

Table 1. Demographic information for research participants

We included participants in this study if they were between 21 and 70 years of age, had a unilateral transtibial amputation (but were not excluded for toe amputations on the contralateral limb), at least 6 months post-amputation at the time of implant, had no serious comorbidities that could increase their risk of participating, were not taking anticoagulant drugs, did not have an MRI-incompatible implanted metal device, and did not have implanted electronic devices such as a pacemaker, defibrillator, or infusion pump. We excluded women who were pregnant or breast feeding. We also excluded people from the 90-day implant study if their hemoglobin A1c level was above 8.0%, due to increased risk of infection associated with hyperglycemia. Each participant's neurological and physiological health was evaluated by a clinician prior to implantation.

Implanting leads for epidural spinal cord stimulation

We implanted SCS leads percutaneously under local and/or twilight anesthesia in a minimally invasive, outpatient procedure. SCS leads were inserted into the dorsal epidural space over the lumbosacral spinal cord using a 14-guage 4-inch epidural Tuohy needle with the participants lying in the prone position. The leads were steered posterior-laterally using a stylet, guided by live fluoroscopy. We aimed to place the electrodes over the caudal lumbosacral enlargement to target the distal dermatome of the residual limb and missing foot. In Participant 1, we implanted three 16-contact leads (Infinion, Boston Scientific, Marlborough, MA); two were near the T12-L2 vertebral levels and the third targeted the cauda equina. In Participant 2, we implanted two 16-

contact leads (Infinion, Boston Scientific, Marlborough, MA) near the T12-L2 vertebral levels. In Participant 3, we implanted three 8-contact leads (Octrode, Abbott Laboratories, Chicago, IL) near the T12-L2 vertebral levels (Fig 1B). We connected each lead to an external stimulator. We stimulated intraoperatively and iteratively adjusted the lead placement based on the participants' verbal report of the location of sensations evoked in the residual limb. We monitored lead location and migration using weekly X-rays for the first 4 weeks (all participants), then twice monthly after that (Participant 3 only) and compared them to the intraoperative fluoroscopic images. In Participant 1, we anchored the leads using sutures to the superficial layers of skin at the exit incisions. All three leads migrated caudally throughout the implant duration. Thereafter, in Participants 2 and 3, we anchored the leads to subcutaneous fascia via a small incision to provide additional stability to the electrode placements. At the end of the study, we removed all percutaneous leads and closed all incision points.

Electromyography procedures

SCS-evoked EMG data were collected during multiple testing sessions across the implantation period. At the beginning of each day of testing, we cleaned and prepared the skin overlying the muscles of both legs using abrasive gel (Lemon Prep, Mavidon, USA) and alcohol wipes (Nuprep, Weaver, Aurora, CO). We placed bipolar pairs of surface EMG electrodes (Ag|AgCl disposable dual EMG electrodes, MVAP Medical, Thousand Oaks, CA) on the following proximal leg muscles bilaterally in all participants: knee extensors (rectus femoris (RF), vastus medialis (VM) and lateralis (VL)), knee flexors (biceps femoris (BF), and semitendinosus (ST)), ankle flexor (tibialis anterior (TA)), and knee extensor (lateral gastrocnemius (LG)) (Figure 1). Based on palpation and guided contraction of the residual muscles in the amputated limb, we placed electrodes on additional ankle extensor muscles: the putative soleus (SO) of Participant 1 and putative medial gastrocnemius (MG) of Participants 2 and 3. The putative SO and MG were determined by palpating the residual limb while instructing the participants to attempt plantarflexion while the knee was flexed (SO) or extended (MG). Here, we sometimes refer to the muscles by grouping them according to their function: knee extensors (BF, ST), knee flexors (RF, VM, VL), ankle extensors (LG, MG, SO), ankle flexors (TA). We placed a ground electrode (Natus Disposable Ground Electrode, MVAP Medical Supplies, CA) on the anterior superior iliac spine ipsilateral to the amputation.

Participants 2 and 3 were tested while standing with support (from a walker or assistive frame) or unassisted during the experiments. Participant 1 had difficulty standing for long durations; therefore, he was either seated or standing, based on his standing tolerance and comfort. We acquired EMG signals at a 30 kHz sampling rate using the Grapevine NIP Neurodata Acquisition System (Ripple, Salt Lake City, UT), with the SurfS2 front-end which has an input range of ±8 mV and 16-bit resolution with 0.25 μV/bit. The SurfS2 includes hardware filters: a 0.1 Hz high pass filter and a 7.5 kHz low pass filter. For participant 3, we used the EMG front-end for the Grapevine system (Sampling rate: 7.5 kHz; Input Range: ± 187.5 mV; ADC: 24-bit resolution with 0.022 μV/bit).

During overground walking experiments, we used wireless data acquisition systems to record EMG signals. In Participant 2, we used the Grapevine NOMAD (Ripple, Salt Lake City, UT) with the SurfS2 front-end. In Participant 3, we used the Trigno Avanti system (Delsys, Natick, MA; sampling rate: 2 kHz; input range: ± 22mV; sensor bandwidth: 10 – 850 Hz).

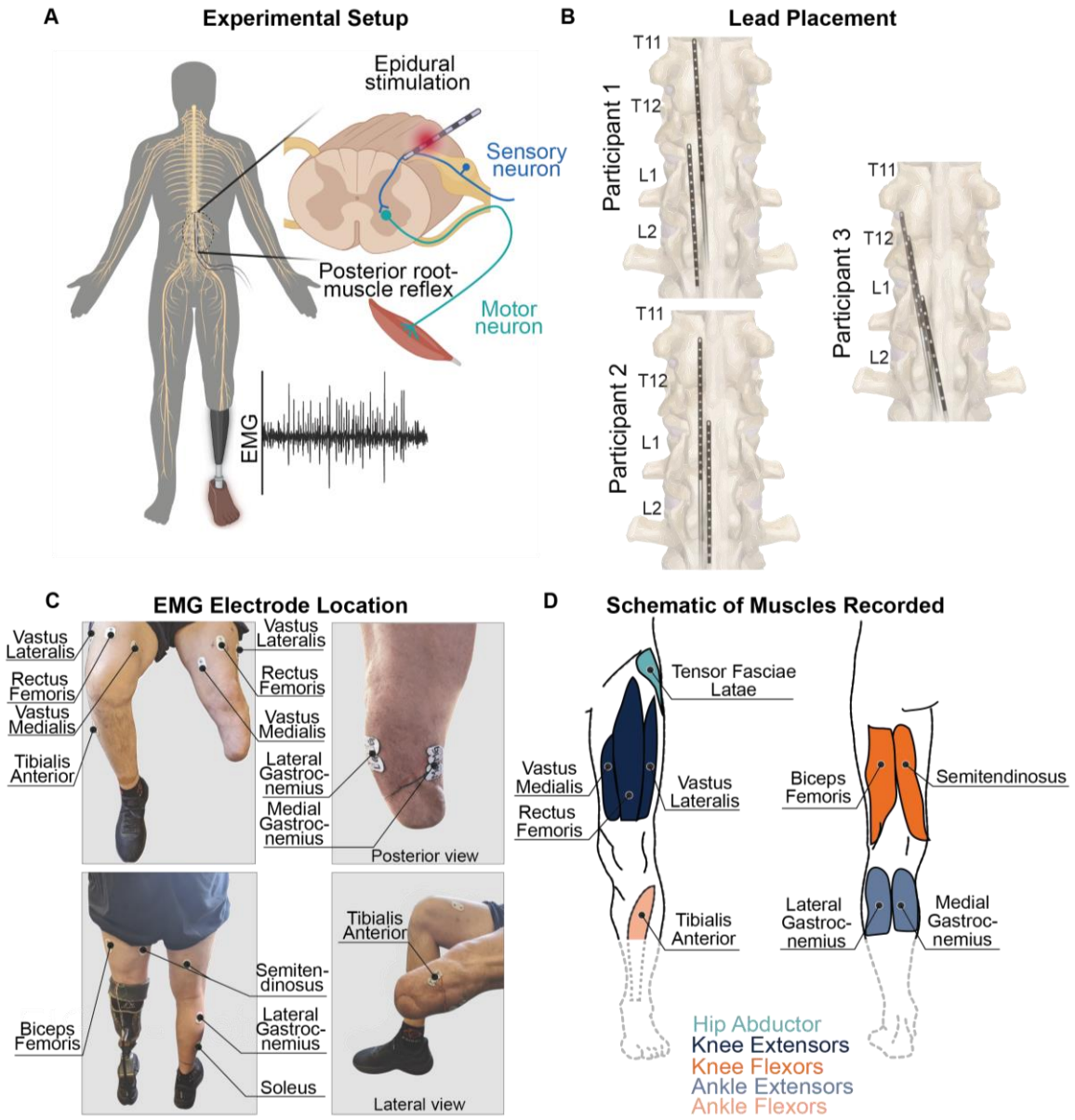

Figure 1. Recording setup and SCS electrode locations. (A) Schematic of the experimental setup. Laterally placed epidural spinal cord stimulation (SCS) leads were placed over the lumbosacral region of the spinal cord. Electromyography (EMG) recorded muscle activity and the posterior root-muscle reflex from the muscles of the residual and intact limbs. (B) Location of the SCS electrodes, as confirmed from X-rays, relative to spinal vertebral segments for all participants at week 1 (Participants 2 and 3) and week 2 (Participant 1) post-implant. (C) EMG electrode locations on the intact and residual limbs in Participant 2. (D) Schematic of the muscles where EMG was recorded for all three participants. Functional groupings of muscles are indicated by color: hip abductor (teal), knee extensors (dark blue), knee flexors (dark orange), ankle extensors (light blue), and ankle flexors (light orange). We recorded tensor fasciae latae from Participant 3 only.

Spinal cord stimulation protocol

Electrical stimulation pulses were delivered using three 32-channel constant current stimulators (Nano 2+Stim; Ripple, Salt Lake City, UT). The maximum current output for these stimulators was 1.5 mA per channel. To achieve the higher current amplitudes required for SCS, we built and used

a custom circuit board to combine the output of groups of four channels. This increased the maximum current output to 6 mA per channel, with 8 effective channels. We used custom software in MATLAB (MathWorks, Natick, MA, USA) to control the SCS. Stimulation pulses were symmetric and charge-balanced, delivered in a monopolar configuration, with an external return electrode (Natus Disposable Ground Electrode, MVAP Medical Supplies, CA) placed over the right acromion. For Participants 1 and 2, the stimulation pulses were anodic-leading. Due to a change in the software that we used to deliver stimulation, in Participant 3, we delivered stimulation as cathodic-leading. However, due to the biphasic symmetric shape of the stimulus waveform, these changes in polarity did not likely affect the PRM responses.

Study session protocol

Participants attended testing sessions 2–4 days per week throughout the implant period. Within these sessions, reflex and EMG measures were collected between 1.5 and 3 days per week across all participants. The rest of the time was spent testing sensory responses to SCS [10].

Detecting responses evoked in muscle

We performed a survey across all electrodes that evoked sensory percepts by delivering 10 pulses at every combination of stimulation amplitude (2 – 6 mA, in 0.5 – 2 mA steps) and pulse width (0.2 – 0.6 ms). For all stimulation parameters tested, we considered an evoked response to be present when the recorded EMG signal exceeded 5 standard deviations (SD) above baseline in the 100 ms following a stimulation pulse. To allow for a range of stimulus amplitudes that were comfortable for the participants, we selected pulse widths of 0.4, 0.5, and 0.2 ms for Participants 1, 2, and 3, respectively.

Recruitment curves

We varied the stimulation amplitude through electrodes that evoked sensory percepts from 0.25 mA (below threshold) to the maximum amplitude tolerated by the participants, in increments of 0.25 or 0.5 mA. We repeated stimulation at each amplitude 15 – 20 times at a rate of 1 Hz and randomized the order of each amplitude tested.

Confirming reflex responses

If the evoked response is reflex-mediated, (i.e., from activation of sensory afferents), then following two consecutive stimuli, the amplitude of the second response will be smaller in amplitude compared to the first response. This phenomenon is referred to as rate-dependent depression (RDD) [18,29,30]. RDD is not observed when the motoneurons are directly activated by the stimulation pulse. Therefore, we sought to confirm that the recorded responses were indeed reflexive by observing RDD. We stimulated with pairs of pulses having interstimulus intervals of 1s, 500 ms, 200 ms, 100 ms, and 50 ms, corresponding to frequencies of 1, 2, 5, 10, and 20 Hz, respectively. This was done for every amplitude tested for the recruitment curves.

Sensory feedback during overground walking

We delivered SCS during walking in Participants 2 and 3 starting on Day 23 and Day 22 post-implant, respectively. We instructed the participants to walk at their self-selected speed across a 6-meter walkway. Wireless plantar pressure sensing insoles (Moticon Insole 3, Munich, Germany) measured limb loading. When the plantar pressure of the insole in the prosthetic foot exceeded a pre-programmed threshold to indicate the stance phase, the stimulation was triggered to evoke sensations in the participant's missing foot. Therefore, SCS was delivered only during the stance phase of the prosthetic limb. Stimuli in Participant 2 were on-off triggered at a constant amplitude

when insole pressure exceeded 35 N/cm^2. For Participant 3, stimulus amplitude was linearly modulated with insole pressure above a threshold of 3 N/cm^2. Stimuli were delivered at 50 Hz for Participant 2 and 90 Hz for Participant 3, with a pulse width of 0.2 ms for both participants. These frequencies were chosen because they evoked reliable sensory percepts and were comfortable for the participants. For Participant 3, we recorded from the tensor fasciae latae (TFL) instead of VM during walking to include a more proximal muscle. We recorded gait kinematics while Participant 3 was walking using a 16-camera OptiTrack motion analysis system (Natural Point, OR, USA). We placed 16 reflective markers on anatomical landmarks according to the OptiTrack "Conventional Lower Body" model [31,32]. We sampled the motion capture data at 100 Hz.

Data analysis methods

To allow for comparisons across participants, we express the stimulus intensity as a unit of charge (C), which was calculated by multiplying the amplitude of the cathodic phase of the stimulus (A) by the pulse width (s).

Measuring muscle recruitment and reflex responses

The EMG data were bandpass filtered from 30 to 800 Hz (4th order Butterworth filter) with a notch filter at 60 Hz. We defined the latency of the PRM reflexes as the time between the stimulation onset and the first peak. To construct the recruitment curves, at each stimulation charge, we calculated the average peak-to-peak amplitude of the PRM reflexes.

We characterized RDD by comparing the peak-to-peak amplitude of the PRM reflexes from successive stimuli. We expressed the peak-to-peak amplitude of the PRM reflex from later stimuli as a percentage of the peak-to-peak amplitude of the first response. We repeated this procedure across all frequencies (1, 2, 5, 10, 20, and 50 Hz).

We characterized the relative activation of the lower-limb muscles across spinal segments at 1 µC for Participant 1, 3 µC for Participant 2, and 1.2 µC for Participant 3. The stimulation charge was selected based on the maximum tolerable charge that could be delivered across a majority of the electrodes. We performed this functional mapping procedure within two days following an X-ray to ensure accurate positioning of the electrodes. The peak-to-peak amplitude of EMG responses for each SCS electrode were standardized using z-scores. We then scaled the standardized values by subtracting all the muscle responses' z-score with the minimum muscle response's z-score across the electrodes. Therefore, a z-score of zero indicated the minimum magnitude of muscle activity for that participant across all electrodes.

Characterizing changes in reflex responses over time

To characterize possible changes in PRM reflex recruitment over time, we selected a low and high stimulation frequency: 1 Hz and 50 Hz. The low frequency of 1 Hz was selected for most PRM reflex analyses. The high frequency of 50 Hz was evaluated because SCS to evoke sensations was delivered at 50 Hz [10]. Participant 1 was excluded from this analysis due to significant lead migration throughout the implant duration. To quantify changes in PRM reflexes over time, we compared the peak-to-peak amplitude of the PRM reflex responses evoked by stimulation through a single electrode at 1 Hz across early and late testing days (Days 10 and 21 for Participant 2; Days 20 and 70 for Participant 3). To compare recruitment curves over time, we expressed the peak-to-peak responses with respect to the stimulation charge normalized to the reflex activation threshold.

During sensory-SCS (50 Hz), participants indicated the location of the perceived sensation on a touchscreen interface [33]. For quantifying changes in PRM reflexes evoked during SCS, we calculated the root mean square (RMS) of the reflex response within a 15 ms-long window, starting 5 ms following the stimulus artefact. Trials with high background EMG activity or high baseline noise were excluded from this analysis. To further ensure that the background activity did not affect the comparison, we subtracted the mean baseline RMS from the EMG RMS during stimulation.

We also sought to compare the change in amplitude of muscle activity evoked by stimulation on electrodes that did or did not evoke sensory percepts in the missing limb over time in Participant 2. Therefore, we compared the change in RMS amplitude of the reflex responses between early and late testing days in each muscle for SCS electrodes that produced sensations in the residual and missing limb (between Day 7 and Day 21) compared to an electrode that produced sensations in the residual limb only (between Day 6 and Day 21). These comparisons were made using identical stimulation parameters (pulse width, amplitude, and frequency) for both electrodes. The thresholds for evoking sensory percepts were the same for both early and late testing days.

Quantifying muscle activity during walking

Participants 2 and 3 were instructed to walk overground at a self-selected speed with and without SCS applied during the stance phase. The stimulation train was delivered at 50 Hz and 90Hz for Participant 2 and 3 respectively, based on the comfort level of the participants. In Participant 2, a PRM reflex was detected during walking, in some cases, in the EMG of VL and RF muscles of the residual limb; the walking EMG data from the other muscles were too noisy to analyze. EMG from the overground walking experiments were high-pass filtered using a 2^{nd} order Butterworth filter with a cut-off frequency of 300 Hz. We determined the PRM reflex latency and amplitude of consecutive responses across a variety of interstimulus intervals (14 - 49 Hz). In Participant 3, we demonstrated alternating activation of the VL muscles from the intact and residual limbs during walking at a self-selected speed with SCS off and on. These EMG data were z-scored to normalize the amplitude for each muscle.

In Participant 3, we sought to quantify any differences in muscle activation amplitude and timing during walking with stimulation at a self-selected speed compared to walking without stimulation. We extracted the EMG envelope by first applying a high-pass filter with a cut-off frequency of 0.1 Hz, then rectifying. We computed the moving average of the rectified signal, using a bin size of 200 samples, followed by calculating the z-score to normalize the amplitude for each muscle. Step cycles were segmented using the TA EMG from the intact limb to detect heel-strike event times. Specifically, we marked 10% of maximal activation of the TA muscle at offset as 20% of the gait cycle, based on previous reports of muscle activation during gait [34,35]. Using that marker, we aligned all EMG data from all muscles accordingly. We calculated the step cycle duration as the time between segmented steps of the intact limb. We compared step cycle duration across conditions using a one-way analysis of variance (ANOVA).

To compare the timing and overall activation of the muscle profiles during walking, we first time-normalized each step to align as 0 – 100% of the gait cycle. We then found the average and standard deviation of the single-step EMG envelopes. Next, we calculated the cross correlation of the average EMG envelopes across conditions. From the cross correlation, we obtained a measure of similarity and a time lag between the two EMG envelopes. Additionally, we determined

the difference in overall muscle activation magnitude by calculating and comparing the area-under-the-curve of the average EMG envelope.

In order to quantify the co-contraction of antagonistic muscles across the knee joint during walking, we calculated the co-contraction area using the integrated activation of the EMG envelopes from the VL and BF muscles across conditions [36,37]:

$$Co - Contraction\ Area = \frac{\int BF}{\int VL} \quad (1)$$

where a larger co-contraction area indicates greater co-contraction of these antagonistic muscles.

Due to an error during data collection, we do not have EMG data for all muscles during walking for Participant 3. Therefore, we were unable to assess co-contractions of the ankle muscles, nor were we able to assess changes in TFL activity in the intact limb. This error has since been mitigated and will not impact future studies.

Gait kinematics

We sought to characterize the functional consequences in muscle activation and timing while Participant 3 was walking at a self-selected speed with stimulation and compared to walking without stimulation. We also characterized the effect of long-term SCS on muscle activation when Participant 3 was walking without stimulation at the early and later timepoints of the implant. Because we observed changes in TFL muscle activity (described in detail below), we measured the pelvic obliquity during walking. Pelvic obliquity is the rotation of the pelvis in the coronal-plane (Figure 8A inset). We filtered the marker positions over time using a fourth order low-pass Butterworth filter (cut-off frequency = 20 Hz). We calculated the pelvic obliquity (θ) of Participant 3 during walking using the left and right anterior superior iliac spine (ASIS) motion capture marker 3-dimensional positions [38]:

$$\theta = \frac{180}{\pi} \times \tan^{-1}\left(\frac{Y_I - Y_R}{\sqrt{(X_I - X_R)^2 + (Z_I - Z_R)^2}}\right) \quad (2)$$

where the *X, Y,* and *Z* coordinates correspond to the medial-lateral, rostral-caudal, and anterior-posterior dimensions, respectively, and *I* and *R* are the intact and residual limb, respectively. When the ASIS markers were equal in elevation, the pelvic obliquity was 0º. When the ASIS marker on the residual limb was tilted higher than the intact limb, the pelvic obliquity was negative. From the pelvic obliquity, we extracted two measures: the range-of-motion and pelvic drop. The range-of-motion is the maximal peak-to-peak value of the pelvic obliquity for a single step (Figure 8). The pelvic drop is the downward rotation angle of the contralateral hip from the time of ipsilateral foot contact to the maximum pelvic obliquity [38]. We measured the pelvic drop for both the intact and residual limbs.

We compared the following conditions for pelvic obliquity: range-of-motion at the early timepoint without SCS, late timepoint without SCS, and late timepoint with SCS. We compared pelvic drop between the intact and residual limbs, and at the early timepoint without SCS, late timepoint without SCS, and late timepoint with SCS. To compare the pelvic obliquity range-of-motion and pelvic drop across conditions, we used a permutation test, which is a non-parametric statistical approach often used for smaller sample sizes [39]. The permutation test entails a resampling

with replacement from the observed data, maintaining the number of measurements in each condition. We obtained 10,000 resampled and shuffled sets of data, and for each set, calculated the difference in means. We compared the difference in means from each of the permutations of the resampled data with the difference in means of the observed data. We obtained a one-sided p-value by calculating the proportion of resampled permutations where the difference in means was greater than the observed mean, and dividing that by the number of repetitions (10,000). We used the Shapiro–Wilk test to test for normality and Levene's test to assess the homogeneity of variance. For all statistical analyses, we considered a p-value < 0.05 to indicate significance.

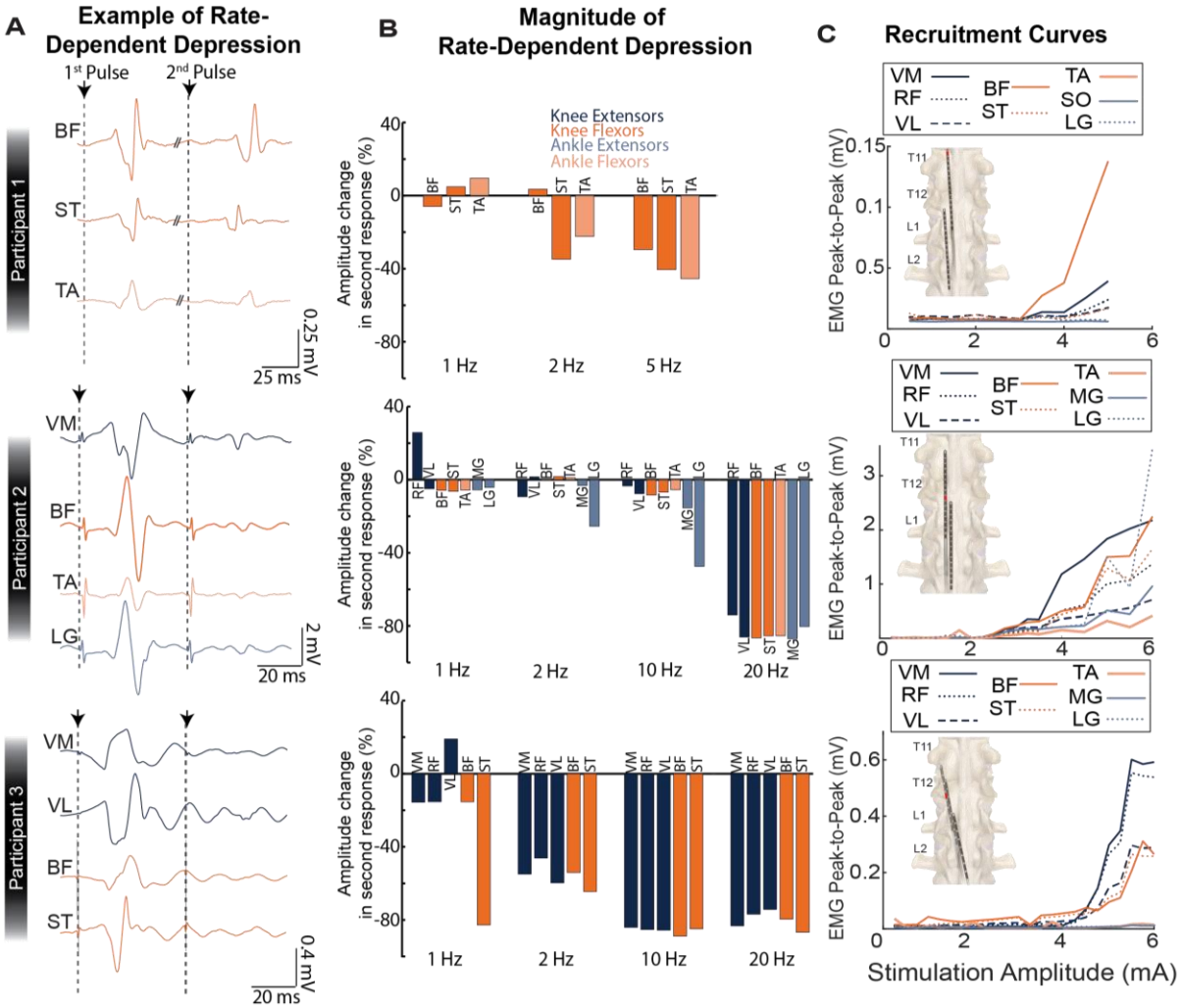

Figure 2. SCS evoked posterior root-muscle (PRM) reflexes. (A) Characteristic PRM reflex responses evoked at 1.5 times reflex threshold with an inter-stimulus interval of 100ms (for Participant 1) and 50ms (for Participant 2 and 3), demonstrating rate-dependent depression (RDD) of the second response compared to the first. (B) The change in the peak-to-peak amplitude of the second response compared to the first response for each muscle where reliable PRM reflexes were evoked in each participant. (C) Examples of recruitment curves when stimulation amplitude was increased through an electrode that evoked sensory percepts in the missing limb (electrode indicated in inset). Muscles are grouped by color: knee extensors (dark blue); knee flexors (dark orange); ankle extensors (light blue); ankle flexor (light orange). VL = vastus lateralis, RF = rectus femoris, VM = vastus medialis, BF = biceps femoris, ST = semitendinosus, TA = tibialis anterior, MG = medial gastrocnemius, LG = lateral gastrocnemius.

RESULTS

SCS evokes posterior root-muscle reflexes in the residual limb

To establish that the responses recorded during SCS were reflexive in nature, we quantified RDD across several interstimulus intervals ranging from 50 ms to 1 s, corresponding to frequencies of 20 Hz to 1 Hz, respectively. RDD of PRM reflexes was present across several muscles in all participants (Figure 2A). At 1 Hz, there was a mix of small magnitude depression and facilitation (< 20% in most instances; Figure 2B). In all participants, as the interstimulus interval decreased (higher frequency), the peak-to-peak amplitude of the second response decreased compared to the first response. At frequencies ≥ 5 Hz (Participant 1), 10 Hz (Participant 2), and 2 Hz (Participant 3), RDD was present in all muscles. At the highest frequency tested (5 Hz for Participant 1, 20 Hz for Participants 2 and 3), the mean (± SD) decrease in the second response compared to the first response was 38.5% (± 8.1%) for Participant 1, 83.6% (± 4.8%) for Participant 2, and 80.14% (± 4.97%) for Participant 3 (Figure 2B).

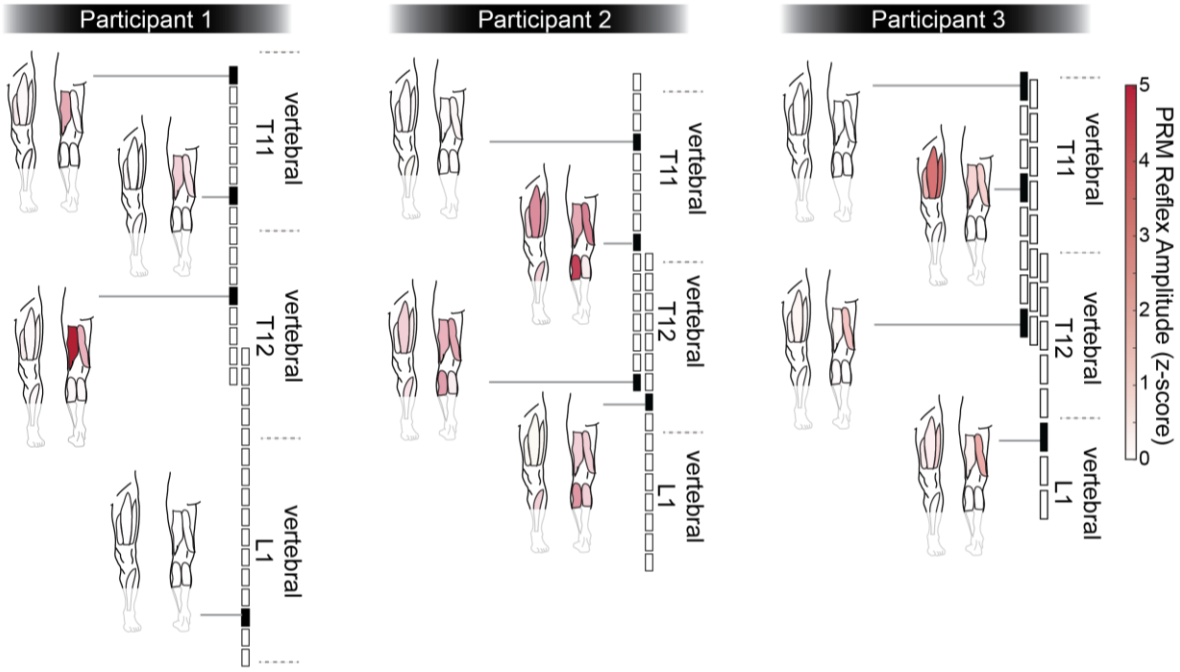

Figure 3. Posterior root-muscle (PRM) reflex peak-to-peak amplitude (z-scored) following stimulation through electrodes according to their rostral-caudal placement over the lumbosacral enlargement.

Characterizing PRM reflex recruitment

We constructed recruitment curves by varying the stimulating amplitude through electrodes that evoked sensory percepts in each participant and measured the peak-to-peak amplitude of the PRM reflex responses (Figure 2C). Nearly all recruitment curves did not reach their saturation point, indicating that the stimulation intensity required to achieve maximal reflex recruitment was greater than 6 mA.

We characterized the relative activation of the muscles of the residual limb according to the rostral-caudal placement of the electrodes over the spinal cord. At the most rostral electrode (near the T11 vertebra), there was absent or minimal activation of the most proximal muscles in all participants (Figure 3). Stimulation through more caudal electrodes exhibited diffuse activation of all muscles in all participants. However, the evoked reflex activity was larger for

muscles in the myotomes corresponding to the location of the SCS electrode. Selective activation of individual muscles was not achieved in any participant or through any electrode.

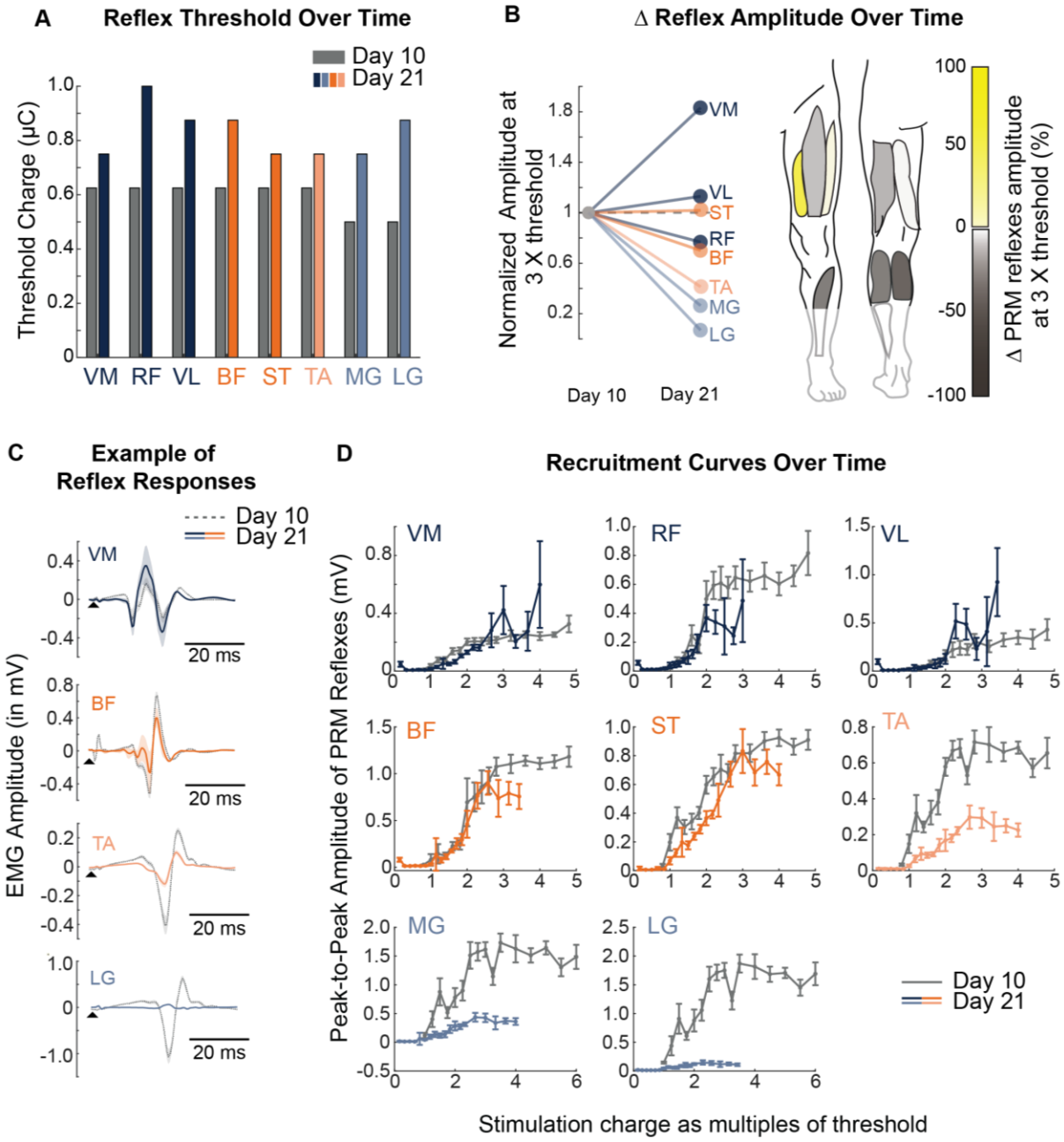

Figure 4. Changes in posterior root-muscle (PRM) reflexes during quiet standing over long-term SCS in Participant 2. (A) Change in PRM reflex threshold over time across muscles. (B) Relative change in PRM reflex amplitude at 3 times threshold between Days 10 and 21. The yellow color bar indicates an increase in reflex amplitude; the grey color bar indicates a decrease in reflex amplitude. (C) Example EMG traces from four muscles stimulated at 3 μC between Day 10 (grey, dashed) and Day 21 (colored, solid). The stimulation onset is indicated with an arrow. (D) Recruitment curves with stimulation amplitude expressed as a multiple of threshold for Day 10 (grey) and Day 21 (colored). VL = vastus lateralis, RF = rectus femoris, VM = vastus medialis, BF = biceps femoris, ST = semitendinosus, TA = tibialis anterior, MG = medial gastrocnemius, LG = lateral gastrocnemius.

Changes in PRM reflex activation over time with SCS

We evaluated the change in the PRM reflex activation during standing over the duration of the implant for Participants 2 and 3 (we excluded Participant 1 from this analysis due to significant lead migration). In both participants, the PRM reflex threshold increased over time for all muscles (Mean ± SD thresholds: Participant 2: Day 10 = 0.6 ± 0.06 µC, Day 21 = 0.8 ± 0.09 µC; Participant 3: Day 29 = 0.9 ± 0.07 µC, Day 70 = 1.3 ± 0.18 µC; Figure 4A; Supplementary Figure 1A). However, the thresholds to evoke sensory percepts did not change (Participant 2: 0.4 µC; Participant 3: 0.6 µC). In addition, we observed an increase in the peak-to-peak amplitude of the PRM reflexes in the knee extensors from Day 10 to Day 21 (24.3% increase for Participant 2 at 3 times reflex threshold; Figure 4B-D; 56.8% increase for Participant 3 at 1.25 times reflex threshold; Supplementary Figure 1B-C). The amplitude of the reflexes in the knee flexors decreased in both Participant 2 (14%) and Participant 3 (27.8%). The amplitude of the reflexes in the ankle flexors (58.7%) and extensors (83.3%) decreased for Participant 2. Participant 3 did not have any activity in the ankle flexors or extensors. Overall, knee extensor amplitude increased, knee flexor amplitude decreased, and the amplitude of the distal muscles either decreased or was absent (Supplementary Table 1).

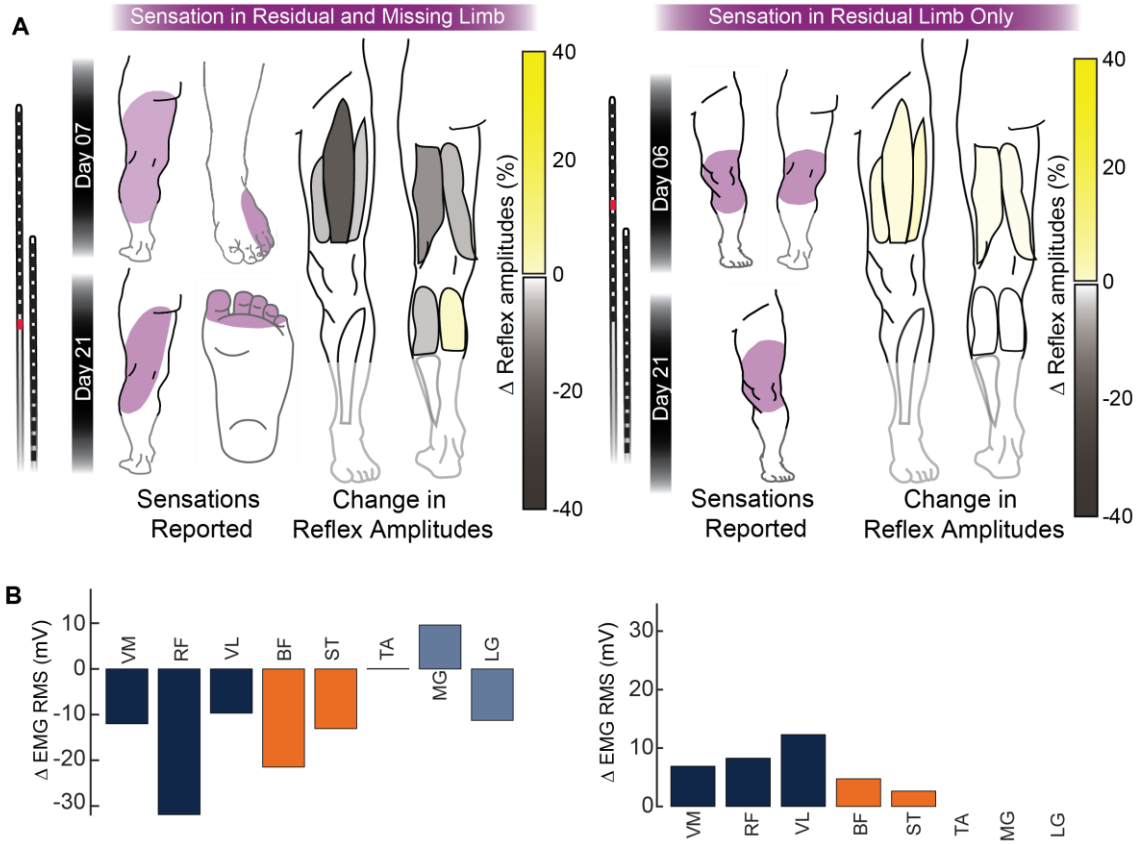

Figure 5. Changes in posterior root-muscle (PRM) reflex amplitudes over time, according to the location of sensory percepts, in Participant 2. (A) Relative change in root mean square (RMS) amplitude of PRM reflexes between Weeks 1 and 3 for an electrode (marked in red) that evoked sensory percepts in the residual and missing limb (left), and an electrode that evoked sensory percepts in the residual limb only (right). (B) Quantification of the change in RMS amplitude of PRM reflexes over time for each muscle. VL = vastus lateralis, RF = rectus femoris, VM = vastus medialis, BF = biceps femoris, ST = semitendinosus, TA = tibialis anterior, MG = medial gastrocnemius, LG = lateral gastrocnemius.

Changes in PRM reflexes when sensory percepts are evoked in the missing limb

To understand possible changes in PRM reflexes in relation to the evoked sensory percepts, we delivered stimulation through an electrode that evoked sensory percepts in the residual limb only, and a different electrode that evoked sensory percepts simultaneously in both the residual and missing limb in Participant 2. The reported sensory percepts from the electrode (near the caudal end of the T12 vertebrae) that produced sensations in the missing and residual limb spanned the posterior side of the residual limb, extending distally, and were stable over time (Day 7 – Day 21; Figure 5A). For that electrode, the RMS amplitude of the PRM reflex response decreased in the knee extensors and flexors as well as LG, with no changes in TA activation. Conversely, the amplitude of the PRM reflex response increased in the MG muscle over time. The sensations produced in the residual limb only resulted from SCS through an electrode near the caudal end of the T11 vertebra and were localized to the anterior and posterior knee (stable from Days 6 – 21; Figure 5A). Stimulation through that electrode produced increases in the RMS amplitude of the PRM reflex response in the knee extensors and flexors and no responses present in the distal muscles. The changes in RMS amplitude of the PRM reflex responses across individual muscles are shown in Figure 5B.

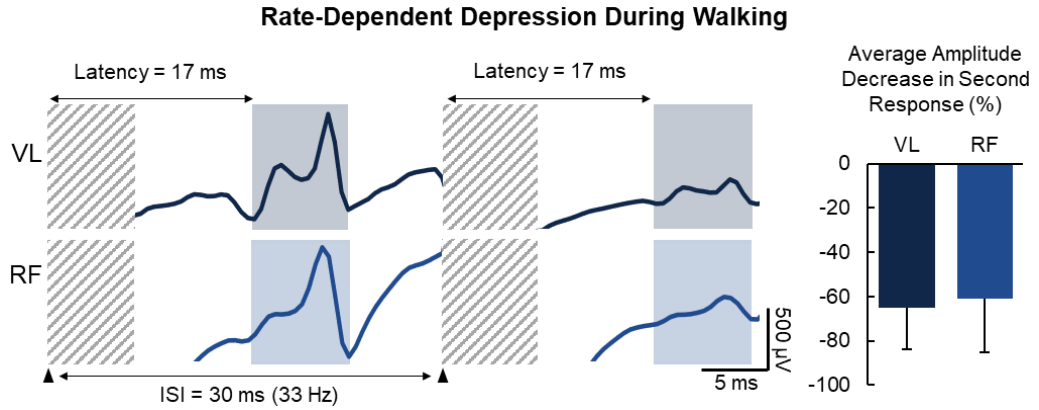

Figure 6. Rate-dependent depression of posterior root-muscle reflexes. (A) Examples in vastus lateralis (VL) and rectus femoris (RF) muscles while Participant 2 walked. Stimulation artefact is covered by gray diagonal lines; PRM reflex is outlined by shaded boxes. (B) Average (–standard deviation) decrease of the second reflex amplitude compared to the first response. ISI = interstimulus interval.

PRM reflexes are present during walking

Participant 2 walked with a step cycle duration of 1.40 ± 0.09 s without stimulation and 1.38 ± 0.1 s with stimulation, which were not significantly different ($p = 1.0$). While Participant 2 was walking with SCS, PRM reflex responses were observable in the residual limb throughout the stimulation train when the interstimulus interval was greater than 20 ms (< 50 Hz). The onset latency of the reflex response in both VL and RF muscles was 17 ms (Figure 6). If PRM reflex responses were observable following the first two consecutive stimulation pulses at the start of the train, they were analyzed for RDD. This occurred 17 times in the EMG of the VL muscle and 11 times in the EMG of the RF muscle. In all instances of two consecutive reflex responses at the start of a stimulation train, the second response was smaller in amplitude than the first response, confirming the presence of RDD. The amplitude of the second response was 65.2% (± 18.7%) and 66.4% (± 25.8%) smaller than the amplitude of the first response for VL and RF, respectively. There was a poor correlation between the interstimulus interval and the decrease in the amplitude of the second reflex response in VL ($R^2 = 0.12$) and RF ($R^2 = 0.32$).

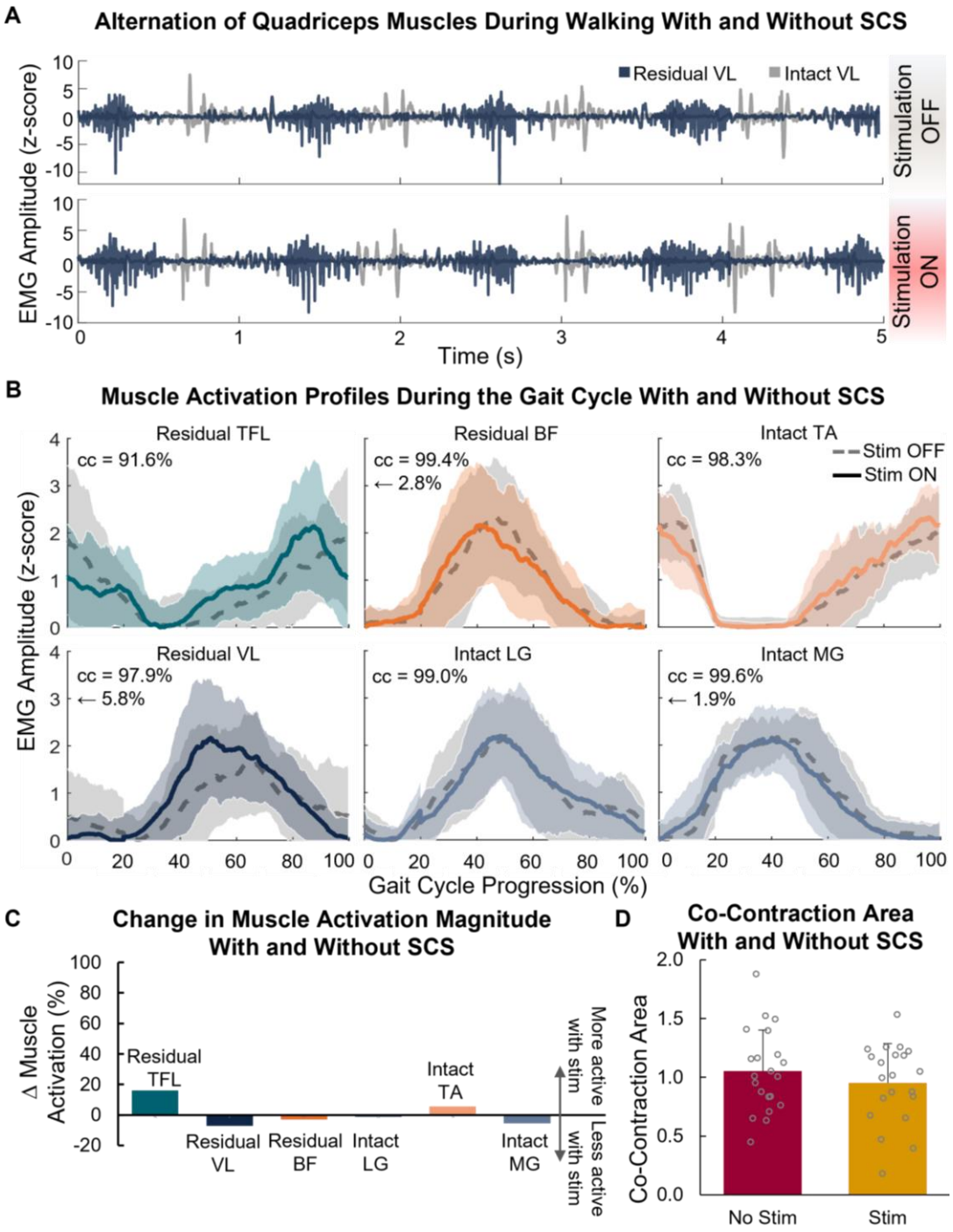

Figure 7. Muscle activity during walking with and without spinal cord stimulation (SCS) in Participant 3 on Day 63. (A) Unfiltered bursts of muscle activity from the alternating residual and intact vastus lateralis (VL) muscles. (B) Mean ± standard deviation (SD) EMG envelopes throughout the gait cycle, with (solid line) and without (dashed line) SCS. Stim = stimulation; cc = cross correlation of the two EMG envelopes; arrow indicates relative shift of EMG envelope with SCS compared to without, expressed as a percentage of gait cycle. TFL = tensor fasciae latae; BF = biceps femoris; LG = lateral gastrocnemius; TA = tibialis anterior; MG = medial gastrocnemius. (C) Change (Δ) in muscle activation amplitude. Positive change = muscle was more active with SCS than without. (D) Mean (+ SD) co-contraction area, indicating co-contractions of BF and VL muscles, with and without SCS.

Hip abductors are more active following multiple weeks of SCS

Participant 3 was implanted for 84 days; therefore, we were able to conduct more trials of walking with sensory feedback over time. Participant 3 walked with a step cycle duration of 1.11 ± 0.36 s at the early timepoint (Day 30) without stimulation, 1.08 ± 0.14 s at the later timepoint (Day 63) without stimulation, and 1.05 ± 0.2 s at the later timepoint (Day 63) with stimulation. These cycle durations were not significantly different ($p = 0.75$). Both the residual and intact VL muscles exhibited alternating bursting activity during walking without and with SCS (Figure 7A). We generated EMG envelope profiles of several muscles across the residual and intact limbs throughout the gait cycle without stimulation over time (Supplementary Figure 2A) and at the later timepoint with and without stimulation (Figure 7B). Overall, the muscle activation profiles with and without SCS at the later time point were similar across all muscles, exhibiting high cross-correlation values (all > 90%; Figure 7B). The residual TFL, intact LG, and intact TA had zero lag between the envelopes, whereas the residual VL, residual BF, and intact MG exhibited small changes in timing: the envelope with SCS was shifted earlier by < 6% of the gait cycle compared to without stimulation. Without SCS at the early and later time points, the residual TFL muscle had moderate cross correlation equal to 72.9% and the rest of the muscles strongly correlated (>96%; Supplementary Figure 2A). The residual TFL and VL muscles were more active at the later timepoint compared to the early time point, with 77.6% and 81.7% increases in amplitude, respectively (Supplementary Figure 2B). The TFL muscle increased in amplitude by a further 16.0% with SCS (Figure 7C). With SCS, the other muscles exhibited small changes in amplitude that were less than 8%.

Co-contractions of knee antagonist muscles are reduced following long-term SCS

For Participant 3, we compared the activation of muscles during walking without sensory stimulation at Days 30 and 63 post-implant, and with and without stimulation at Day 63 (sensory feedback testing during walking began on Day 23 post-implant). At the early timepoint without SCS, there was a high co-contraction area between the VL and BF muscles of the residual limb during walking (co-contraction area = 1.57 ± 0.52; Supplementary Figure 2D). At the later timepoint, the co-contraction area reduced significantly to 1.05 (±0.35; $p < 0.001$) without stimulation and 0.95 (± 0.33; $p < 0.001$; Figure 7D) with stimulation, indicating that undergoing multiple weeks of SCS was associated with reduced co-contraction between the knee antagonist muscles of the residual limb, with a further reduction in co-contraction when SCS was turned on.

Pelvic obliquity range-of-motion and pelvic drop increase following long-term SCS

The large change in residual TFL activity over time may be indicative of plastic changes in the sensorimotor networks in the spinal cord as a result of repeated exposure to SCS over multiple weeks. Therefore, we analyzed motion capture data from the same walking trials to determine the functional consequences of the additional TFL activation during the stance phase of the residual limb. Specifically, we measured the pelvic obliquity during walking (Figure 8A). The pelvic obliquity range-of-motion at the early timepoint without stimulation was 8.08º (± 1.55º) (Figure 8B). At the later timepoints, the range-of-motion increased to 9.20º (± 1.69º) and 8.80º (± 0.91º), without and with SCS, respectively. The increase in range-of-motion at the later timepoint with SCS was significantly different from the early timepoint without SCS ($p = 0.027$). The range-of-motion at the later timepoint without SCS was not different from the early timepoint without SCS ($p = 0.065$) nor the later timepoint with SCS ($p = 0.212$). Overall, the pelvic drop of the residual limb was significantly smaller than the intact limb ($p = 0.002$; Figure 8B). The pelvic drop of the

residual limb increased significantly from 3.62° (± 1.04°) at the early timepoint to 4.76° (± 1.53°) at the later time point without SCS (p = 0.022). Furthermore, the pelvic drop of the residual limb was significantly higher at the later timepoint with SCS (4.46° ± 1.04°) compared to the early timepoint without SCS (p = 0.034). The pelvic drop at the later timepoint with and without SCS were not significantly different (p = 0.258). Therefore, the increase in TFL activity with SCS corresponded to functional improvements in pelvic obliquity range-of-motion and pelvic drop.

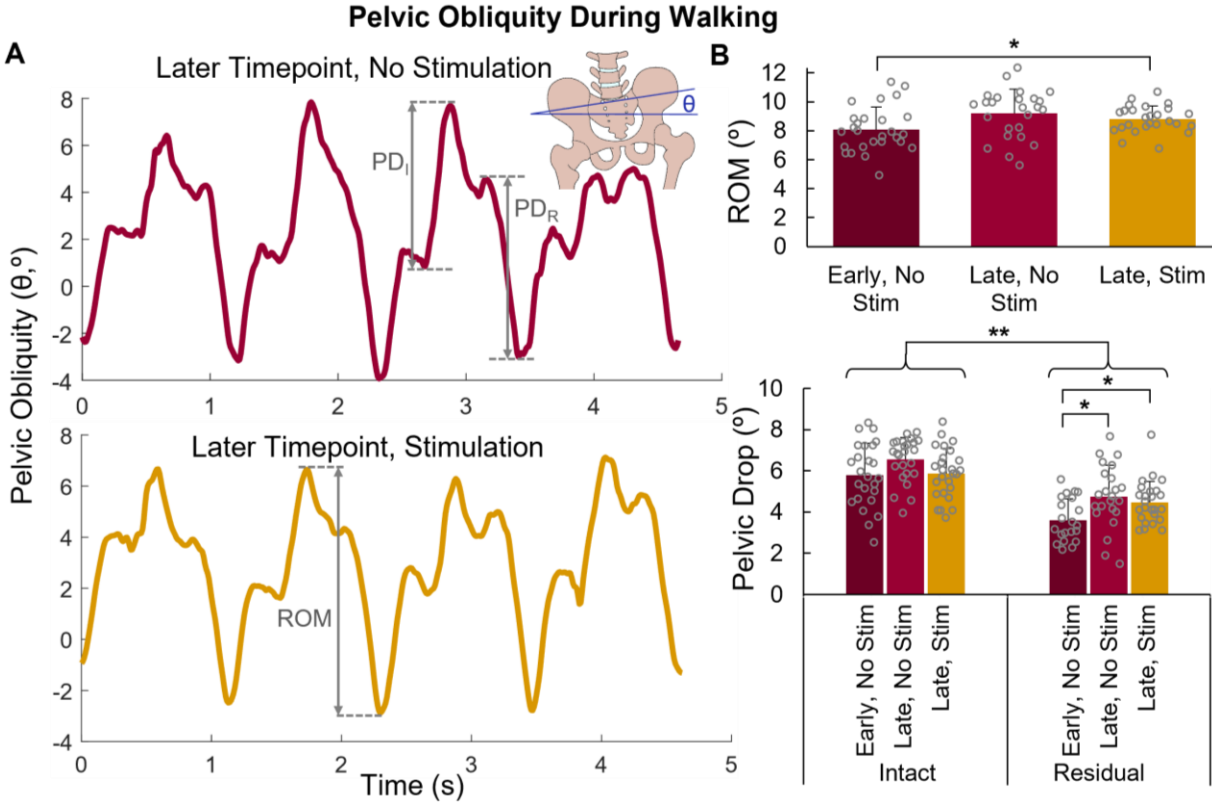

Figure 8. Pelvic obliquity during walking. (A) Examples of pelvic obliquity (θ) without spinal cord stimulation (SCS) (top) and with SCS (bottom) at Day 63. The inset depicts an illustration of pelvic obliquity. The pelvic drop (PD) is the downward rotation angle of the contralateral hip from the time of ipsilateral foot contact to the maximum pelvic obliquity. The range-of-motion (ROM) is the peak-to-peak amplitude of the pelvic obliquity for a single step. I = intact limb, R = residual limb. (B) ROM (top) and PD (bottom) at the early (Day 30) and later timepoints without SCS, and the later timepoint with SCS. *p < 0.05; **p < 0.01.

DISCUSSION

Our previous work showed that SCS can be used to evoke sensory percepts in a missing limb [10,40,41]. However, sensorimotor networks are highly integrated, especially in the spinal cord, via reflexive pathways. Activation of spinal reflex pathways using SCS can elicit changes in muscle activation following neural injury [42,43]. The primary goal of this study was to characterize the muscle activity evoked via spinal reflex pathways from SCS in people with trans-tibial amputations. Changes in muscle activity following extended exposure to SCS corresponded with functional improvements in hip motion and reduced co-contractions of knee antagonist muscles.

Posterior root-muscle reflexes are present following limb amputation

Two of our participants had diabetic neuropathy. In diabetic neuropathy, tendon tap and Hoffman (H-) reflexes are prolonged or absent [44,45]. Conversely, painful diabetic neuropathy presents with the opposite effect, where H-reflexes are exaggerated and RDD is impaired [46–48]. Participant 3 had painful diabetic neuropathy prior to their amputation. In our experience, H-reflexes are difficult, if not impossible, to evoke in people with a lower-limb amputation, regardless of whether a neuropathy is present or not [49]. SCS targets the dorsal spinal roots, exciting large diameter afferent fibers [15,50]. Therefore, PRM reflexes consist of a superposition of H-reflexes and cutaneous afferent inputs [19,20,51]. Here, we present and characterize PRM reflexes evoked using SCS in people with a lower-limb amputation, with and without diabetic neuropathy. We were able to evoke PRM reflexes in all participants. Furthermore, RDD of the PRM reflexes was present in all participants, including during walking, demonstrating that stimulation was not directly activating motor neurons in the ventral spinal cord or roots. We have previously shown that PRM reflexes can be evoked using transcutaneous spinal cord stimulation (tSCS) in people with transtibial amputations with and without diabetic neuropathy [49]. tSCS is a non-invasive stimulation technique that uses electrodes placed on or adjacent to the spine [18,52]. tSCS excites the same afferent fibers as SCS [53]. tSCS and SCS enable the study of spinal reflexes while avoiding the peripheral sensory nerve component. This is beneficial because distal sensory nerve fibers are most susceptible to metabolic stressors from diabetes since the dorsal root ganglia lie outside of the blood-brain barrier [54]. Therefore, studying the recruitment properties of PRM reflexes in people with a limb amputation and/or diabetes presents a novel way to examine the excitability of the spinal cord in each of these populations, as well as following the application of a therapy, such as SCS or tSCS.

Muscle recruitment following limb amputation and SCS

When stimulating at any location in the lumbosacral enlargement, we observed broad recruitment of muscles in the residual limb, with the strongest activation corresponding to the relevant myotome. This broad recruitment may have occurred because of a number of factors, including current spread in the cerebrospinal fluid (CSF) exciting multiple spinal root segments [55], the activation of intraspinal networks [56,57], or due to plastic changes in the spinal circuitry following limb amputation [58]. The latter is the most likely explanation. While current spread through the CSF can lead to the activation of multiple spinal root segments [55], this spread would not likely affect all spinal roots of the lumbosacral enlargement. Similarly, the activation of intraspinal networks connecting several motoneuron pools throughout the lumbosacral enlargement can contribute to multi-joint movements [56,57]; however, these movements typically consist of functional synergies, such as flexion or extension synergies, which would not lead to broad activation of all lower-limb muscles. A study in non-human primates showed that, following limb amputation, the motoneurons innervating the distal muscles survive, and that they reinnervate different muscle targets in the residual limb [58]. This expansion in the motor unit innervation is a possible reason for the broad muscle recruitment with SCS shown here, especially in Participant 2, who had a traumatic amputation. This may also explain why, despite targeting sensations in the distal limb, there are changes in proximal muscle activation during standing and walking after long-term SCS. This may be influenced by possible length-dependent degeneration of nerve fibers that is typical in people with diabetic neuropathy [59,60].

When sensory percepts were present in the missing limb (in addition to the residual limb), there was an increase in the PRM reflex amplitude of the MG muscle and decreased amplitude in all proximal muscles over time. When sensory percepts were in the residual limb only, there was an increase in the PRM reflex amplitude of the proximal muscles over time. It appears that PRM reflex activation may correspond to the location of the sensory percepts; however, this finding could only be observed in a single participant. Future studies should further characterize the relationship between changes in PRM reflex activation and the location of sensory percepts.

Restoring sensation improves joint stability and range of motion during walking

People who use a leg prosthesis exhibit a host of gait abnormalities, arising in part from the loss of sensation from the missing limb, reducing their confidence in weight-bearing on the prosthetic limb. As a result, prosthesis users will employ compensatory movements to increase their stability and confidence as they walk. For example, knee flexors and extensors of the residual limb co-contract more than the intact limb during walking in people with trans-tibial amputations [37]. Co-contraction of antagonistic muscles about the knee is a compensatory strategy to increase stiffness in preparation for foot-contact and weight-bearing. Prosthesis users will also exhibit exaggerated hip hiking (raised hip) or circumduction (abduction and semi-circular movement) of the prosthetic limb during the swing phase to ensure that the foot clears the ground [38]. These compensatory hip movements stem from insufficient residual limb knee bending and lack of ankle dorsiflexion during swing, resulting in toe dragging, which could cause tripping. Pelvic obliquity is a measure of pelvic rotation in the coronal-plane and can be used to indicate hip hiking [38]. Specifically, during the stance phase of walking, hip abductors on the stance leg contract to tilt the pelvis and raise the contralateral hip to aid with foot clearance, resulting in an increased pelvic obliquity. At heel strike, there are small changes in pelvic obliquity, suggestive of improved shock absorption [61]. People with a lower-limb amputation exhibit a reduced pelvic obliquity range-of-motion during gait, with a further decrease in range-of-motion for higher-level amputations [38]. Furthermore, the pelvic drop of the stance limb is smaller on the prosthetic limb than the intact limb [38]. In this study, at the later timepoint with and without SCS, the pelvic drop of the residual limb became more symmetrical with the intact limb. Additionally, at the later timepoint with and without SCS, the pelvic drop of the residual limb increased towards values seen in neurologically-intact adults (5 - 7°; [38])

We demonstrated that SCS activates spinal sensorimotor reflex pathways during walking. It is possible that, by activating these reflex pathways, SCS modulates muscle activity to provide additional and necessary joint stabilization during walking [21–23]. SCS was delivered only during the stance phase of the prosthetic limb, and we found the most drastic change in VL and TFL activity during this phase. The VL muscle is a knee extensor and provides stability to the knee joint during the stance phase. At the later timepoint in the study, the residual VL muscle was more active than the early timepoint. Furthermore, the residual BF muscle was slightly less active at the later timepoint in the study compared to the early timepoint in the study. The increase in VL activity and decrease in BF activity reflect the reduced co-contraction area of the residual limb during walking at the later timepoint. Therefore, instead of excessive co-contraction of the antagonistic muscles to provide stability to the knee joint, knee stability was driven primarily by the VL muscle following SCS. The TFL muscle is a hip abductor; during the stance phase, the TFL muscle contracts, dropping the ipsilateral pelvis, allowing the contralateral pelvis to raise and the contralateral foot to clear the ground [62]. Our results at the early timepoint align with the previous

study showing a decrease in pelvic obliquity range-of-motion and pelvic drop of the residual limb [38]. At the later timepoint, the increased activation of the residual TFL muscle during the stance phase with and without SCS is indicated by the increased pelvic drop and pelvic obliquity range-of-motion. Therefore, we demonstrate that following long-term SCS, there are functional improvements in dynamic stability at the knee and the hip during walking. The functional improvements in pelvic drop were present at the later timepoint, even without stimulation, suggesting a possible rehabilitative effect of SCS on muscle activation and knee and hip motion during walking, but data from additional participants is needed to be conclusive. This study is the first to investigate changes in muscle activity alongside the functional outcomes following long-term use of a sensory neuroprosthesis.

Limitations

We report the recruitment of PRM reflexes by SCS in three people with a trans-tibial amputation with and without diabetic neuropathy. Two participants received 28-day percutaneous implants, and one participant received an 84-day percutaneous implant. During the first few weeks of the study, much of the time was spent characterizing the sensory percepts in the missing limb. Therefore, closed-loop studies with SCS during walking were limited to the last week of the implant (Participant 2) for the 28-day study. More extensive closed-loop sensory feedback testing was possible with Participant 3; therefore, our analyses related to changes in muscle activity during gait were restricted to a single subject. Nonetheless, we demonstrate reduced co-contractions of knee antagonist muscles and improved pelvic obliquity range-of-motion and pelvic drop following extended presentation of SCS. Future studies will build on the current work to further characterize the functional improvements and corresponding changes in muscle activity during walking with long-term SCS.

Participant 1 had difficulty standing for extended durations; therefore, much of the sensory testing and PRM reflex data were collected during sitting in a chair. The data for Participants 2 and 3 were collected during standing. Irrespective of these postural differences, we have shown that SCS could evoke PRM reflexes in all participants. Similarly, other studies using tSCS have shown recruitment of PRM reflexes with varying postures [63,64]. In the future, we aim to systematically characterize the effect of posture on PRM reflexes evoked by SCS.

The participants in this study were heterogeneous, with differing causes of their amputations and their ambulation levels. Despite this heterogeneity, we were able to evoke sensory percepts in all of their missing limbs, as well as elicit PRM reflexes, and demonstrate functional improvements during walking in a participant with diabetic neuropathy. Therefore, our results provide a preliminary demonstration of the broad utility of SCS for sensory restoration, in addition to its prior uses for reducing chronic pain and improving mobility.

Clinical relevance

SCS is a common method to reduce pain, with as many as 50,000 people receiving a SCS implant per year to treat chronic pain [65]. Through our previous work and the current study, we demonstrate that, in addition to reducing phantom limb pain, SCS can be used to restore sensation in the missing limb, improve function during walking [10], and engage spinal reflexes that work to stabilize the residual limb, particularly the knee and pelvis, during walking. Therefore, with improved sensorimotor function, over time, SCS may be able to reduce the incidence of falls

in people with lower limb amputation. Future studies will focus on additional gait tasks and the role of reflex recruitment and muscle activation on improvements in gait over time.

CONCLUSIONS

SCS to restore sensation in the missing limb of people with trans-tibial amputations evoked PRM reflexes in the residual limb. SCS broadly activated the muscles of the residual limb in all the participants. Long-term SCS during walking reduced co-contractions of the knee antagonist muscles and increased activation of the tensor fasciae latae muscle, corresponding to increased pelvic obliquity range-of-motion and pelvic drop. Using a sensory neuroprosthesis modulates spinal reflex activity and muscle activation in the residual limb, leading to functional improvements during walking.

LIST OF ABBREVIATIONS

SCS: spinal cord stimulation

PRM: posterior root-muscle

EMG: electromyography

RF: rectus femoris

VM: vastus medialis

VL: vastus lateralis

BF: biceps femoris

ST: semitendinosus

TA: tibialis anterior

LG: lateral gastrocnemius

MG: medial gastrocnemius

SO: soleus

SD: standard deviation

RDD: rate-dependent depression

TFL: tensor fasciae latae

RMS: root-mean square

ASIS: anterior superior iliac spine

tSCS: transcutaneous spinal cord stimulation

CSF: cerebrospinal fluid

ACKNOWLEDGMENTS

The authors would like to express our sincerest gratitude to our research participants for their time and dedication to furthering the field of neuroprosthetics. We would like to thank Debbie Harrison, Casey Konopisos, and Alayna Schwerer for their assistance with the IRB protocol, clinical trial registration, IDE application, and participant recruitment. Figure 1A was created with BioRender.com

FUNDING SOURCE

This study was funded by the National Institutes of Health (NINDS Award number UH3NS100541 and NICHD Award Number F30HD0987984).

CLINICAL TRIAL INFORMATION

This study was registered under clinical trials NCT03027947 and NCT04547582.

COMPETING INTERESTS

MC and DJW are founders and shareholders of Reach Neuro, Inc.; DJW is a consultant and shareholder of Neuronoff, Inc.; DJW is a shareholder and scientific board member for NeuroOne Medical, Inc.; DJW is a shareholder of Bionic Power Inc., and Iota Biosciences Inc. The other authors declare no conflicts of interests in relation to this work.

REFERENCES

1. Ziegler-Graham K, MacKenzie EJ, Ephraim PL, Travison TG, Brookmeyer R. Estimating the Prevalence of Limb Loss in the United States: 2005 to 2050. 2008;89:422–9.

2. Geiss LS, Li Y, Hora I, Albright A, Rolka D, Gregg EW. Resurgence of Diabetes-Related Nontraumatic Lower-Extremity Amputation in the Young and Middle-Aged Adult U.S. Population. Diabetes Care. 2019;42:50–4.

3. Hunter SW, Batchelor F, Hill KD, Hill A-M, Mackintosh S, Payne M. Risk Factors for Falls in People With a Lower Limb Amputation: A Systematic Review. PM R. 2017;9:170-180.e1.

4. Chihuri S, Wong CK. Factors associated with the likelihood of fall-related injury among people with lower limb loss. Inj Epidemiol. 2018;5:42.

5. Steinberg N, Gottlieb A, Siev-Ner I, Plotnik M. Fall incidence and associated risk factors among people with a lower limb amputation during various stages of recovery - a systematic review. Disabil Rehabil. 2019;41:1778–87.

6. Anderson CB, Miller MJ, Murray AM, Fields TT, So NF, Christiansen CL. Falls After Dysvascular Transtibial Amputation: A Secondary Analysis of Falling Characteristics and Reduced Physical Performance. PM R. 2021;13:19–29.

7. Ortiz-Catalan M, Håkansson B, Brånemark R. An osseointegrated human-machine gateway for long-term sensory feedback and motor control of artificial limbs. Sci Transl Med. 2014;6:257re6.

8. Petrini FM, Bumbasirevic M, Valle G, Ilic V, Mijović P, Čvančara P, et al. Sensory feedback restoration in leg amputees improves walking speed, metabolic cost and phantom pain. Nat Med. 2019;25:1356–63.

9. Charkhkar H, Christie BP, Triolo RJ. Sensory neuroprosthesis improves postural stability during Sensory Organization Test in lower-limb amputees. Sci Rep. 2020;10:6984.

10. Nanivadekar AC, Bose R, Petersen BA, Okorokova EV, Sarma D, Farooqui J, et al. Spinal cord stimulation restores sensation, improves function, and reduces phantom pain after transtibial amputation [Internet]. medRxiv; 2022 [cited 2022 Oct 5]. p. 2022.09.15.22279956. Available from: https://www.medrxiv.org/content/10.1101/2022.09.15.22279956v1

11. Krainick JU, Thoden U, Riechert T. Pain reduction in amputees by long-term spinal cord stimulation. Long-term follow-up study over 5 years. J Neurosurg. 1980;52:346–50.

12. Viswanathan A, Phan PC, Burton AW. Use of spinal cord stimulation in the treatment of phantom limb pain: case series and review of the literature. Pain Pract. 2010;10:479–84.

13. Petersen BA, Nanivadekar AC, Chandrasekaran S, Fisher LE. Phantom limb pain: peripheral neuromodulatory and neuroprosthetic approaches to treatment. Muscle Nerve. 2019;59:154–67.

14. Caylor J, Reddy R, Yin S, Cui C, Huang M, Huang C, et al. Spinal cord stimulation in chronic pain: evidence and theory for mechanisms of action. Bioelectron Med. 2019;5.

15. Greiner N, Barra B, Schiavone G, Lorach H, James N, Conti S, et al. Recruitment of upper-limb motoneurons with epidural electrical stimulation of the cervical spinal cord. Nat Commun. 2021;12:435.

16. Minassian K, Jilge B, Rattay F, Pinter MM, Binder H, Gerstenbrand F, et al. Stepping-like movements in humans with complete spinal cord injury induced by epidural stimulation of the lumbar cord: electromyographic study of compound muscle action potentials. Spinal Cord. 2004;42:401–16.

17. Minassian K, Persy I, Rattay F, Pinter MM, Kern H, Dimitrijevic MR. Human lumbar cord circuitries can be activated by extrinsic tonic input to generate locomotor-like activity. Hum Mov Sci. 2007;26:275–95.

18. Dalrymple AN, Hooper CA, Kuriakose MG, Capogrosso M, Weber DJ. Using a high-frequency carrier does not improve comfort of transcutaneous spinal cord stimulation. J Neural Eng. 2023;20:016016.

19. Krenn M, Toth A, Danner SM, Hofstoetter US, Minassian K, Mayr W. Selectivity of transcutaneous stimulation of lumbar posterior roots at different spinal levels in humans. Biomed Tech (Berl). 2013;58 Suppl 1.

20. Freitas RM de, Capogrosso M, Nomura T, Milosevic M. Preferential activation of proprioceptive and cutaneous sensory fibers compared to motor fibers during cervical transcutaneous spinal cord stimulation: a computational study. J Neural Eng. 2022;19:036012.

21. Strange KD, Hoffer JA. Restoration of use of paralyzed limb muscles using sensory nerve signals for state control of FES-assisted walking. IEEE Trans Rehabil Eng. 1999;7:289–300.

22. Prochazka A, Ellaway P. Sensory systems in the control of movement. Compr Physiol. 2012;2:2615–27.

23. Dalrymple AN, Mushahwar VK. Stimulation of the Spinal Cord for the Control of Walking. Neuroprosthetics [Internet]. World Scientific; 2017. p. 811–49. Available from: http://www.worldscientific.com/doi/abs/10.1142/9789813207158_0025

24. Capaday C, Stein RB. Amplitude modulation of the soleus H-reflex in the human during walking and standing. J Neurosci. 1986;6:1308–13.

25. Stephens MJ, Yang JF. Short latency, non-reciprocal group I inhibition is reduced during the stance phase of walking in humans. Brain Res. 1996;743:24–31.

26. Pearson KG. Proprioceptive regulation of locomotion. Curr Opin Neurobiol. 1995;5:786–91.

27. Prochazka A, Westerman RA, Ziccone SP. Ia afferent activity during a variety of voluntary movements in the cat. J Physiol. 1977;268:423–48.

28. Fitzpatrick RC, Taylor JL, McCloskey DI. Ankle stiffness of standing humans in response to imperceptible perturbation: reflex and task-dependent components. J Physiol (Lond). 1992;454:533–47.

29. Hultborn H, Illert M, Nielsen J, Paul A, Ballegaard M, Wiese H. On the mechanism of the post-activation depression of the H-reflex in human subjects. Exp Brain Res. 1996;108:450–62.

30. Hofstoetter US, Freundl B, Binder H, Minassian K. Recovery cycles of posterior root-muscle reflexes evoked by transcutaneous spinal cord stimulation and of the H reflex in individuals with intact and injured spinal cord. PLoS ONE. 2019;14:e0227057.

31. Petersen BA, Sparto PJ, Fisher LE. Clinical measures of balance and gait cannot differentiate somatosensory impairments in people with lower-limb amputation. Gait & Posture. 2023;99:104–10.

32. OptiTrack. OptiTrack Wiki - NaturalPoint Product Documentation Ver 2.2 [Internet]. 2022 [cited 2023 Sep 8]. Available from: https://v22.wiki.optitrack.com/index.php?title=OptiTrack_Wiki

33. Nanivadekar A, Chandrasekaran S, Gaunt R, Fisher L. RNEL PerceptMapper [Internet]. Zenodo; 2020 [cited 2023 Mar 7]. Available from: https://zenodo.org/record/3939658

34. Yang JF, Winter DA. Surface EMG profiles during different walking cadences in humans. Electroencephalogr Clin Neurophysiol. 1985;60:485–91.

35. Winter DA, Yack HJ. EMG profiles during normal human walking: stride-to-stride and inter-subject variability. Electroencephalogr Clin Neurophysiol. 1987;67:402–11.

36. Damiano DL, Martellotta TL, Sullivan DJ, Granata KP, Abel MF. Muscle force production and functional performance in spastic cerebral palsy: relationship of cocontraction. Arch Phys Med Rehabil. 2000;81:895–900.

37. Seyedali M, Czerniecki JM, Morgenroth DC, Hahn ME. Co-contraction patterns of trans-tibial amputee ankle and knee musculature during gait. J Neuroeng Rehabil. 2012;9:29.

38. Michaud SB, Gard SA, Childress DS. A preliminary investigation of pelvic obliquity patterns during gait in persons with transtibial and transfemoral amputation. J Rehabil Res Dev. 2000;37:1–10.

39. Pesarin F, Salmaso L. The permutation testing approach: a review. Statistica. 2010;70:481–509.

40. Chandrasekaran S, Nanivadekar AC, McKernan G, Helm ER, Boninger ML, Collinger JL, et al. Sensory restoration by epidural stimulation of the lateral spinal cord in upper-limb amputees. Makin TR, Ivry RB, Makin TR, Perich MG, editors. eLife. 2020;9:e54349.

41. Nanivadekar AC, Chandrasekaran S, Helm ER, Boninger ML, Collinger JL, Gaunt RA, et al. Closed-loop stimulation of lateral cervical spinal cord in upper-limb amputees to enable sensory discrimination: a case study. Sci Rep. 2022;12:17002.

42. Wagner FB, Mignardot J-B, Le Goff-Mignardot CG, Demesmaeker R, Komi S, Capogrosso M, et al. Targeted neurotechnology restores walking in humans with spinal cord injury. Nature. 2018;563:65–71.

43. Powell MP, Verma N, Sorensen E, Carranza E, Boos A, Fields D, et al. Epidural stimulation of the cervical spinal cord improves voluntary motor control in post-stroke upper limb paresis [Internet]. medRxiv; 2022 [cited 2022 Jul 21]. p. 2022.04.11.22273635. Available from: https://www.medrxiv.org/content/10.1101/2022.04.11.22273635v1

44. Hendriksen PH, Oey PL, Wieneke GH, Bravenboer B, Banga JD. Subclinical diabetic neuropathy: similarities between electrophysiological results of patients with type 1 (insulin-dependent) and type 2 (non-insulin-dependent) diabetes mellitus. Diabetologia. 1992;35:690–5.

45. Millán-Guerrero R, Trujillo-Hernández B, Isais-Millán S, Prieto-Díaz-Chávez E, Vásquez C, Caballero-Hoyos JR, et al. H-reflex and clinical examination in the diagnosis of diabetic polyneuropathy. J Int Med Res. 2012;40:694–700.

46. Lee-Kubli CAG, Calcutt NA. Altered rate-dependent depression of the spinal H-reflex as an indicator of spinal disinhibition in models of neuropathic pain. Pain. 2014;155:250–60.

47. Marshall AG, Lee-Kubli C, Azmi S, Zhang M, Ferdousi M, Mixcoatl-Zecuatl T, et al. Spinal Disinhibition in Experimental and Clinical Painful Diabetic Neuropathy. Diabetes. 2017;66:1380–90.

48. Lee-Kubli C, Marshall AG, Malik RA, Calcutt NA. The H-Reflex as a Biomarker for Spinal Disinhibition in Painful Diabetic Neuropathy. Curr Diab Rep. 2018;18:1.

49. Dalrymple AN, Fisher LE, Weber DJ. Transcutaneous Spinal Cord Stimulation to Reduce Phantom Limb Pain in People with a Transtibial Amputation [Internet]. medRxiv; 2023 [cited 2023 Apr 19]. p. 2023.04.13.23288483. Available from: https://www.medrxiv.org/content/10.1101/2023.04.13.23288483v1

50. Capogrosso M, Wenger N, Raspopovic S, Musienko P, Beauparlant J, Bassi Luciani L, et al. A computational model for epidural electrical stimulation of spinal sensorimotor circuits. J Neurosci. 2013;33:19326–40.

51. Minassian K, Persy I, Rattay F, Dimitrijevic MR, Hofer C, Kern H. Posterior root-muscle reflexes elicited by transcutaneous stimulation of the human lumbosacral cord. Muscle Nerve. 2007;35:327–36.

52. Barss TS, Parhizi B, Mushahwar VK. Transcutaneous spinal cord stimulation of the cervical cord modulates lumbar networks. Journal of Neurophysiology. 2019;jn.00433.2019.

53. Hofstoetter US, Freundl B, Binder H, Minassian K. Common neural structures activated by epidural and transcutaneous lumbar spinal cord stimulation: Elicitation of posterior root-muscle reflexes. PLoS ONE. 2018;13:e0192013.

54. Feldman EL, Nave K-A, Jensen TS, Bennett DLH. New Horizons in Diabetic Neuropathy: Mechanisms, Bioenergetics, and Pain. Neuron. 2017;93:1296–313.

55. Holsheimer J. Computer modelling of spinal cord stimulation and its contribution to therapeutic efficacy. Spinal Cord. 1998;36:531–40.

56. Dalrymple AN, Everaert DG, Hu DS, Mushahwar VK. A speed-adaptive intraspinal microstimulation controller to restore weight-bearing stepping in a spinal cord hemisection model. J Neural Eng. 2018;15:056023.

57. Giszter SF. Motor primitives--new data and future questions. Curr Opin Neurobiol. 2015;33:156–65.

58. Wu CW, Kaas JH. Spinal cord atrophy and reorganization of motoneuron connections following long-standing limb loss in primates. Neuron. 2000;28:967–78.

59. Callaghan BC, Cheng HT, Stables CL, Smith AL, Feldman EL. Diabetic neuropathy: clinical manifestations and current treatments. The Lancet Neurology. 2012;11:521–34.

60. Watson JC, Dyck PJB. Peripheral Neuropathy: A Practical Approach to Diagnosis and Symptom Management. Mayo Clin Proc. 2015;90:940–51.

61. Kaufman K, Sutherland D. Kinematics of normal human walking. Human Walking. 3rd ed. Philadelphia: : Lippincott Williams & Wilkins; 2006. p. 33–51.

62. Gottschall JS, Okita N, Sheehan RC. Muscle activity patterns of the tensor fascia latae and adductor longus for ramp and stair walking. Journal of Electromyography and Kinesiology. 2012;22:67–73.

63. Danner SM, Krenn M, Hofstoetter US, Toth A, Mayr W, Minassian K. Body Position Influences Which Neural Structures Are Recruited by Lumbar Transcutaneous Spinal Cord Stimulation. PLoS One. 2016;11:e0147479.

64. Roy FD, Gibson G, Stein RB. Effect of percutaneous stimulation at different spinal levels on the activation of sensory and motor roots. Exp Brain Res. 2012;223:281–9.

65. Kumar K, Rizvi S. Historical and present state of neuromodulation in chronic pain. Curr Pain Headache Rep. 2014;18:387.

SUPPLEMENTARY ITEMS

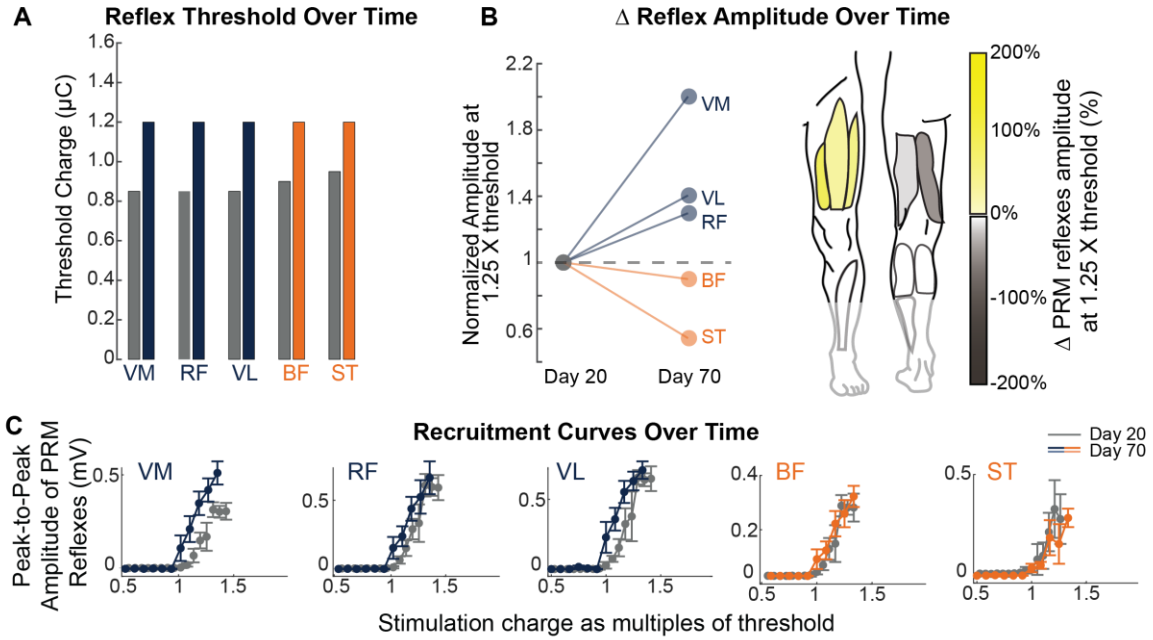

Supplementary Figure 1. Change in posterior root-muscle (PRM) reflex activation over time across muscles for Participant 3. (A) Change in PRM reflex amplitude at 1.5 times threshold between Days 20 and 70. (B) Relative change in PRM reflex amplitude between Days 20 and 70. The yellow color bar indicates an increase in PRM reflex amplitude over time. The grey color bar indicates a decrease in reflex amplitude. (C) Change in PRM reflex threshold over time across muscles. (D) Recruitment curves shown as the fraction of threshold between the two days. VL = vastus lateralis, RF = rectus femoris, VM = vastus medialis, BF = biceps femoris, ST = semitendinosus, TA = tibialis anterior, MG = medial gastrocnemius, LG = lateral gastrocnemius.

Muscle	Participant 2			Participant 3		
	Early time point (mV)	Late time point (mV)	Difference (%)	Early time point (mV)	Late time point (mV)	Difference (%)
Vastus Medialis	0.23	0.42	83.16	0.20	0.39	100.18
Rectus Femoris	0.63	0.49	-23.27	0.37	0.48	29.76
Vastus Lateralis	0.28	0.32	12.99	0.41	0.58	40.47
Biceps Femoris	1.09	0.76	-29.89	0.26	0.24	-9.99
Semitendinosus	0.82	0.83	1.88	0.28	0.15	-45.66
Tibialis Anterior	0.71	0.29	-58.64	-	-	-
Medial Gastrocnemius	1.61	0.43	-73.62	-	-	-
Lateral Gastrocnemius	1.75	0.12	-93.06	-	-	-

Supplementary Table 1. PRM reflex peak-to-peak amplitude across muscles at 3 times (Participant 2) and 1.25 times (Participant 3) the threshold at an early and late timepoint (Participant 2: Day 10 and 21, Participant 3: Day 20 and 70).

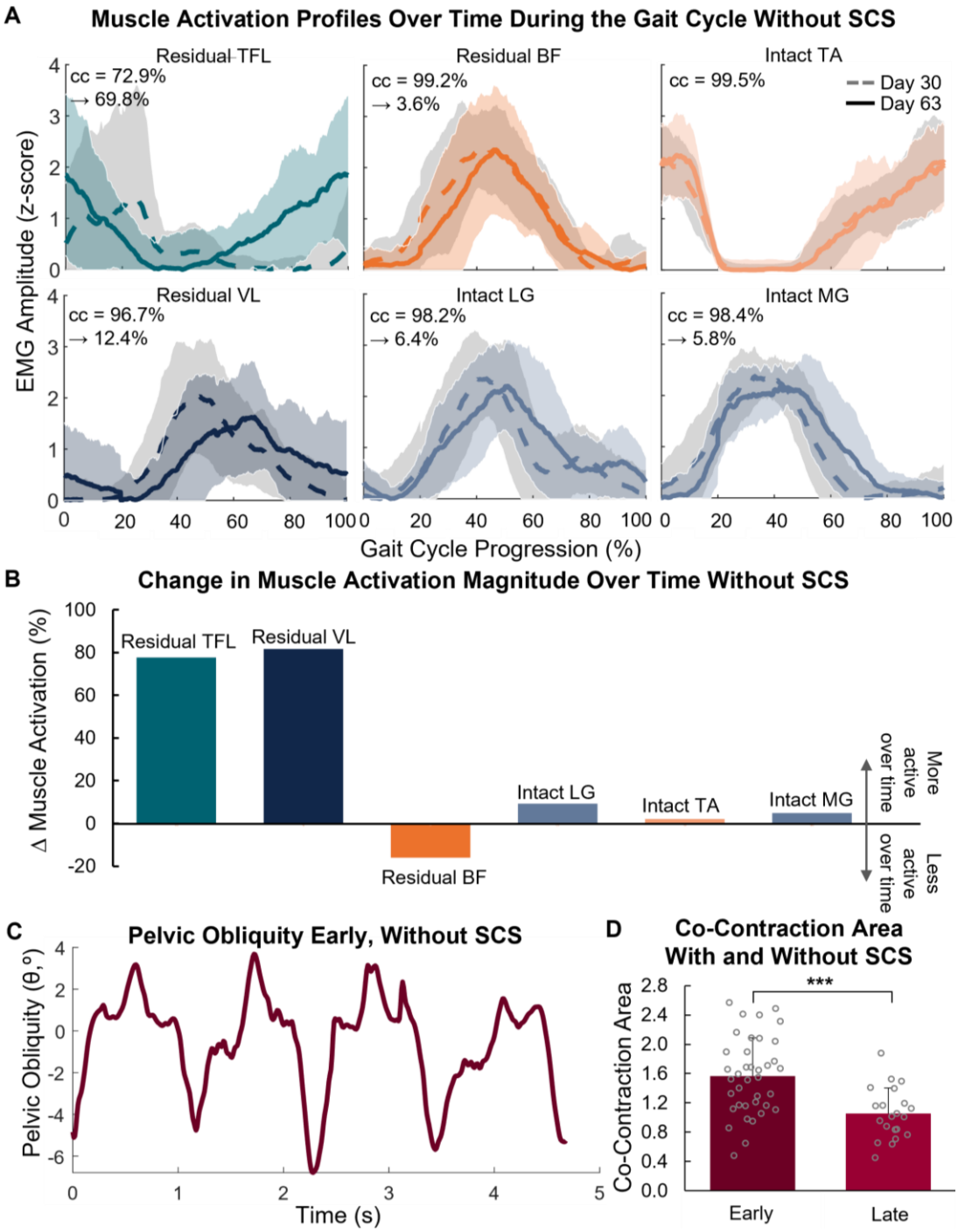

Supplementary Figure 2. Muscle activity during walking over time without spinal cord stimulation (SCS) for Participant 3. (A) Mean ± standard deviation (SD) EMG envelopes of muscles from the residual and intact limbs throughout the gait cycle on Day 30 (dashed) and Day 63 (solid). cc = cross correlation of the two EMG envelopes; arrow indicates relative shift of EMG envelope of the later timepoint compared to the earlier timepoint, expressed as a percentage of the gait cycle. TFL = tensor fasciae latae; VL = vastus lateralis; BF = biceps femoris; LG = lateral gastrocnemius; TA = tibialis anterior; MG = medial gastrocnemius. (B) Change (Δ) in muscle activation amplitude. A positive change means that the muscle was more active at the later timepoint compared to the earlier timepoint. (D) Mean (+ SD) co-contraction area, indicating co-contractions of BF and VL muscles.